Chapter 6
Arraying Techniques

At least five different arraying schemes can be employed in designing an arraying system. In this discussion, they are referred to as full-spectrum combining (FSC), complex-symbol combining (CSC), symbol-stream combining (SSC), baseband combining (BC), and carrier arraying (CA). In addition, sideband aiding (SA) also can be employed, even though it is not strictly an arraying technique since it employs a single antenna (SA uses an estimate of the carrier phase derived from a Costas loop tracking the data sidebands to aid the carrier-tracking loop). In the next few sections, we will discuss how each of these schemes function and attempt to clarify their advantages and disadvantages. Furthermore, in Chapter 7, we will discuss combinations of these schemes, such as carrier arraying with sideband aiding and baseband combining (CA/SA/BC) or carrier arraying with symbol-stream combining (CA/SSC), to determine if such combinations provide any further advantage. The effective symbol SNR is derived for each arraying scheme, assuming L antennas and accounting for imperfect synchronization. In the cases where adjustments in both phase and delay are required to achieve synchronization, the delay component will be assumed as known. This is nominally true because the delay is largely determined by geometry and, therefore, can be accurately estimated. Also, since the signal bandwidths are narrow relative to their transmitted frequency, the delay accuracy is not as critical as is the phase. Complexity versus performance is traded off throughout the chapter, and benefits to the reception of existing spacecraft signals are discussed.

In what follows, the performances of different arraying schemes are compared on the basis of degradation only, since this parameter provides sufficient indication for relative comparison. For an exact performance

prediction, loss should be used in the region where loss and degradation do not agree.

6.1 Full-Spectrum Combining (FSC)

Full-spectrum combining is an arraying technique wherein the signals are combined at IF, as depicted in Figs. 6-1 and 6-2 [1]. One receiver chain—consisting of one carrier, one subcarrier, and one symbol-synchronization loop—then is used to demodulate the combined signal. The combining at IF is two-dimensional in the sense that both delay and phase alignment are required to coherently add the signals. Let the received signal at antenna 1 be denoted by $s_1(t)$. Then, from Eq. (5.1-1), we have

$$s_1(t) = \sqrt{2P_1}\sin\left[\omega_c t + \theta_1(t)\right] \tag{6.1-1}$$

where $\theta_1(t) = \theta_m(t) + \theta_c(t)$. The first term on the right-hand side is $\theta_m(t) = \Delta d(t)\,Sqr\left[\omega_{sc}t + \theta_{sc}\right]$ and represents the data modulation. The second term is $\theta_c(t) = \theta_d(t) + \theta_{osc}(t)$ and represents dynamics and phase noise, with $\theta_d(t)$ being the Doppler due to spacecraft motion and $\theta_{osc}(t)$ the oscillator phase noise. The received signals at the other antennas are delayed versions of $s_1(t)$ and are given by

$$s_i(t) = s(t-\tau_i) = \sqrt{2P_i}\sin\left[\omega_c(t-\tau_i) + \theta_i(t)\right] \tag{6.1-2}$$

for $i = 2,\ldots,L$, where τ_i denotes the delay in signal reception between the first and the ith antenna ($\tau_1 = 0$) and $\theta_i(t) = \theta_1(t-\tau_i) + \Delta\theta_i(t)$. Here, $\Delta\theta_i(t)$ accounts for differential Doppler and phase noises, which typically are "very small." Complex downconverting each $s_i(t)$ signal to IF, we obtain

$$\mathbf{x}_i(t) = \sqrt{P_i}\,e^{j[\omega_I t - \omega_c\tau_i + \theta_i(t)]} \tag{6.1-3}$$

where ω_I denotes the IF frequency. Delaying each $\mathbf{x}_i(t)$ signal by $-\tau_i$ (which is assumed to be known precisely), we have

$$\mathbf{y}_i(t) = \mathbf{x}_i(t+\tau_i) = \sqrt{P_i}\,e^{j\left[\omega_I t + (\omega_I - \omega_c)\tau_i + \theta_1(t) + \Delta\theta_i(t)\right]} \tag{6.1-4}$$

The signals $\mathbf{y}_i(t)$ cannot be added coherently because the phases are not aligned [due to the factor $(\omega_I - \omega_c)\tau_i$ and $\Delta\theta_i$], even though the data symbols are aligned [note that Doppler phase $\theta_d(t)$ is part of $\theta_1(t)$]. Therefore, an additional phase adjustment is necessary to add the signals coherently.

Let us consider an antenna interferometric pair as illustrated in Fig. 6-3. The signal at antenna i arrives τ_i seconds later than the signal at antenna 1,

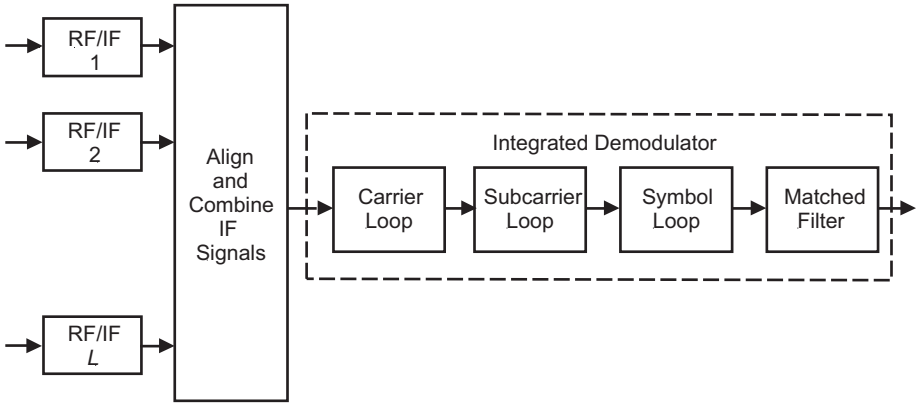

Fig. 6-1. Full-spectrum combining (FSC) for an *L*-antenna array.

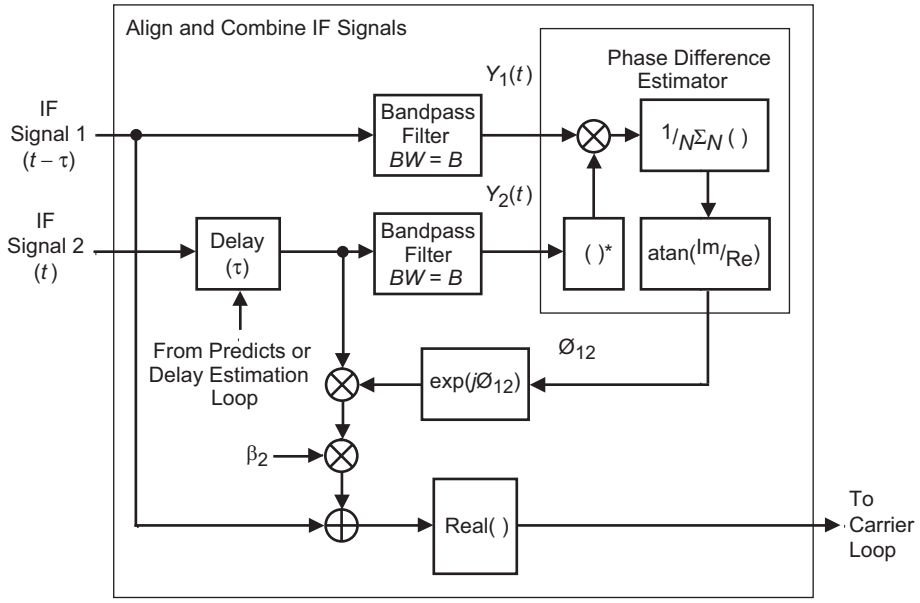

Fig. 6-2. FSC align and combine for a two-antenna array.

which will be used as a reference for mathematical convenience. After low-noise amplification, the signals are downconverted to IF, where the *i*th signal is delayed by $-\tau_i$ seconds. The latter delay consists of two components, a fixed component and a time-varying component. The fixed component compensates for unequal waveguide and cable lengths between the two antennas and the correlator. It is a known quantity that is determined by calibration. The time-

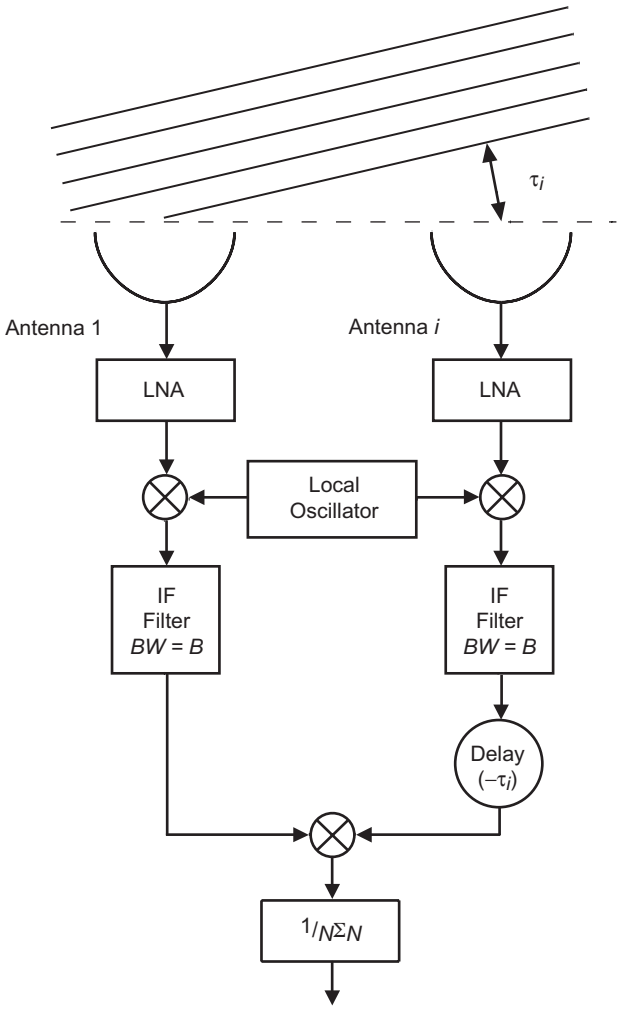

Fig. 6-3. An interferometric pair.

varying component compensates for unequal propagation lengths for the two received signals. This component typically is precomputed from the trajectory of the spacecraft and the physical location of the two antennas. The relative phase difference between the signals is estimated by performing a complex correlation on the resulting signals, which, for all practical purposes, have been aligned in time. At the input to the correlator, the two complex signals from the first and the ith antennas are passed through filters with bandwidth B Hz and subsequently sampled at the Nyquist rate of $2B$ samples per second. Mathematically, the complex sampled signals are given by

$$\mathbf{y}_1(t_k) = \sqrt{P_1}\, e^{j[\omega_I t_k + \theta_1(t_k)]} + \mathbf{n}_1(t_k)$$

and (6.1-5)

$$\mathbf{y}_i(t_k) = \sqrt{P_i}\, e^{j[\omega_I t_k + (\omega_I - \omega_c)\tau_i + \theta_i(t_k)]} + \mathbf{n}_i(t_k)$$

where $\mathbf{n}_1(t_k)$ and $\mathbf{n}_i(t_k)$ are independent complex Gaussian random variables with variances $\sigma_1^2 = N_{01}B$ and $\sigma_i^2 = N_{0i}B$. It will be shown later that the parameter B is essential in determining the averaging period and, thus, the combining loss. Correlating the signals (i.e., multiplying and low-pass filtering), we obtain

$$\mathbf{z}'_{i1}(t_k) = \sqrt{P_1 P_i}\, e^{j[\phi_{i1}(t_k)]} + \mathbf{n}_{i1}(t_k) \tag{6.1-6}$$

where $\phi_{i1} = (\omega_I - \omega_c)\tau_i + \Delta\theta_i(t_k)$ denotes the total phase difference between the signals, and $\mathbf{n}_{i1}$, the effective noise, is given by

$$\begin{aligned}\mathbf{n}_{i1} = {} & \sqrt{P_i}\, e^{j[\omega_I t_k + (\omega_I - \omega_c)\tau_i + \theta_i(t_k)]}\, \mathbf{n}_1(t_k) \\ & + \sqrt{P_1}\, e^{-j[\omega_I t_k + \theta_1(t_k)]}\, \mathbf{n}_i(t_k) + \mathbf{n}_1(t_k)\mathbf{n}_i(t_k)\end{aligned} \tag{6.1-7}$$

with effective variance

$$\sigma^2_{z',i} = \sigma_1^2 P_i + \sigma_i^2 P_1 + \sigma_1^2 \sigma_i^2 = B(N_{01}P_i + N_{0i}P_1 + N_{01}N_{0i}B) \tag{6.1-8}$$

Following the correlation, an averaging operation over T seconds is performed to reduce the noise effect. In that period, N=$2BT$ independent samples are used to reduce the variance of Eq. (6.1-8) by a factor of N. The SNR of $\mathbf{z}_{i1} = (1/N)\sum_{k=1}^{N} \mathbf{z}'_{i1}(t_k)$ at the output of the accumulator, SNR_{i1}, thus is given by

$$\mathrm{SNR}_{i1} = \frac{\mathrm{E}(\mathbf{z}_{i1})\mathrm{E}(\mathbf{z}^*_{i1})}{Var(\mathbf{z}_{i1})} = \frac{N P_1 P_i}{\sigma^2_{zi}} = \frac{P_1}{N_{01}} \frac{2T}{[1 + (1/\gamma_i) + (B N_{0i}/P_i)]} \tag{6.1-9}$$

where γ_i is given by

$$\gamma_i = \frac{P_i}{P_1}\frac{N_{01}}{N_{0i}}\,, \qquad \sum_{i=1}^{L} \gamma_i = \Gamma \tag{6.1-10}$$

and is a function of the receiving antenna only. Appendix D provides these factors for the various DSN antennas at both 2.3 GHz (S-band) and X-band. (Note that, in radio metric applications [2], the SNR is defined as the ratio of

the standard deviation of the signal to that of the noise and is the square root of the SNR defined in the above equation.) When the correlation bandwidth B is very large (in the MHz range), the signal × noise term $(P_1\sigma_i^2 + P_i\sigma_1^2)$ can be ignored, and the effective noise variance is dominated by the noise × noise term $(\sigma_1^2\sigma_i^2)$, i.e.,

$$\sigma_{\mathbf{z}i}^2 \approx \sigma_1^2\sigma_i^2 \tag{6.1-11}$$

In this case, the SNR can be approximated by

$$\mathrm{SNR}_{i1} \approx \frac{P_1}{N_{01}}\frac{P_i}{N_{0i}}\frac{2T}{B} \tag{6.1-12}$$

An estimate of $\phi_{i1}, \hat{\phi}_{i1}$ is obtained by computing the inverse tangent of the real and imaginary parts of $\mathbf{z}_{i1}$, i.e.,

$$\hat{\phi}_{i1} = \tan^{-1}\left[\frac{\mathrm{Imag}[\mathbf{z}_{i1}]}{\mathrm{Real}[\mathbf{z}_{i1}]}\right] \tag{6.1-13}$$

The probability density function of the phase estimate is given in [2] as

$$p(\hat{\phi}_{i1}) = \frac{1}{2\pi}e^{-\mathrm{SNR}_{i1}/2}\left[1 + G\,e^{G^2}\sqrt{\pi}\,(1 + erf(G))\right] \tag{6.1-14}$$

where

$$G = \sqrt{\frac{\mathrm{SNR}_{i1}}{2}}\cos(\hat{\phi}_{i1} - \phi_{i1}) \tag{6.1-15}$$

The density in Eq. (6.1-14) is plotted in Fig. 6-4, and its derivation assumes that the noise $\mathbf{n}_{i1}$ is Gaussian (even though it is not Gaussian in the strict sense, a Gaussian approximation still is justified by invoking the central limit theorem due to the averaging over N samples). Figure 6-4 clearly indicates that a reasonably good phase estimate can be obtained for SNR_{i1} as low as 6 dB. At a moderately high SNR_{i1}, the distribution can be approximated by a Gaussian distribution with variance

$$\sigma_{\hat{\phi}_{i1}}^2 = \frac{1}{\mathrm{SNR}_{i1}} \tag{6.1-16}$$

In the simplest form of FSC, the signal from antenna 1 is correlated with all other signals and the phase errors estimated. An improvement in phase-error

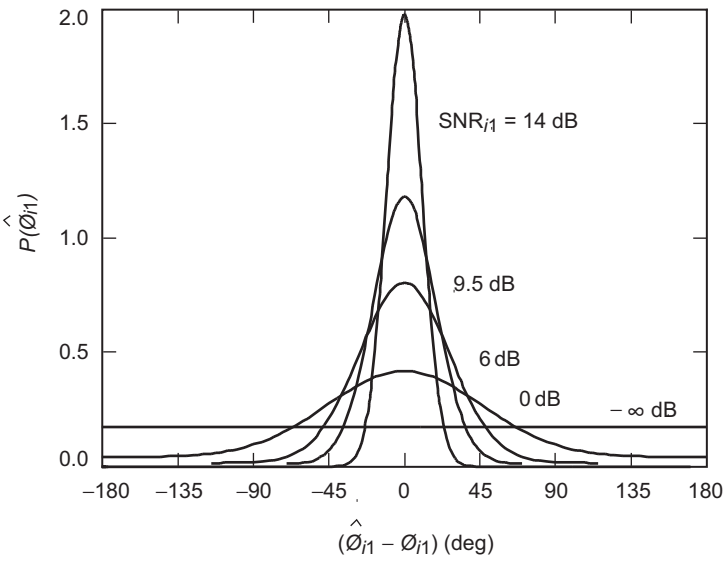

Fig. 6-4. The probability distribution of measured phase as a function of $(\hat{\phi}_{i1} - \phi_{i1})$ for a number of SNRs.

estimation can be obtained by performing global phasing between L antennas, which involves $L(L-1)/2$ complex correlations as the signal from each antenna is correlated with the signal from every other antenna [2]. In addition, closed-loop techniques can be utilized to reduce the phase error, as illustrated in Appendix E.

6.1.1 Telemetry Performance

In order to compute the degradation due to FSC, consider the IF signals after phase compensation, i.e.,

$$\mathbf{y}_i(t_k) = \sqrt{P_i}e^{j[\omega_I t_k + \theta_1(t_k) + \Delta\phi_{i1}(t_k)]} + \mathbf{n}_i(t_k)e^{j[\omega_I t_k + \theta_1(t_k) + \hat{\phi}_{i1}(t_k)]} \qquad (6.1\text{-}17)$$

where $\Delta\phi_{i1} = \hat{\phi}_{i1} - \phi_{i1}$ refers to the residual phase error between antenna 1 and the ith signal, and $\mathbf{n}_i(t_k)$ is the complex envelope of the thermal noise with two-sided noise spectral density N_{0i}. The signal combiner performs the weighted sum of $\mathbf{y}_i(t_k)$, namely

$$\begin{aligned}\mathbf{y}(t_k) &= \sum_{i=1}^{L} \beta_i \mathbf{y}_i(t_k) \\ &= \sum_{i=1}^{L} \beta_i \left[\sqrt{P_i}e^{j[\omega_I t_k + \theta_1(t_k) + \Delta\phi_{i1}(t_k)]} + \mathbf{n}_i(t_k)e^{j[\omega_I t_k + \theta_1(t_k) + \hat{\phi}_{i1}(t_k)]}\right]\end{aligned} \qquad (6.1\text{-}18)$$

Letting $\beta_1 = 1$ and optimizing $\beta_i, i = 2,...,L$, in order to maximize SNR′, we obtain

$$\beta_i = \sqrt{\frac{P_i}{P_1}} \frac{N_{01}}{N_{0i}} \tag{6.1-19}$$

Note that the variance of the combined complex signal $\mathbf{y}(t_k)$ is

$$\sigma_{\mathbf{y}}^2 = B \sum_{i=1}^{L} \beta_i^2 N_{0i} \tag{6.1-20}$$

The total signal power at the output of the combiner conditioned on residual phases, $\Delta\phi_{i1}(t_k)$, thus is given by

$$\begin{aligned} P'_{\mathbf{y}} &= \left[\overline{\left(\mathbf{y}(t_k) \mid \Delta\phi_{i1}(t_k) \right)} \right]^2 \\ &= \sum_{i=1}^{L} \sum_{j=1}^{L} \beta_i \beta_j \sqrt{P_i P_j}\, \mathbf{c}_{IF_i} \mathbf{c}^*_{IF_j} \\ &= \sum_{i=1}^{L} \beta_i^2 P_i + \sum_{i=1}^{L} \sum_{\substack{j=1 \\ i \neq j}}^{L} \beta_i \beta_j \sqrt{P_i P_j}\, \mathbf{c}_{IF_i} \mathbf{c}^*_{IF_j} \end{aligned} \tag{6.1-21}$$

where

$$\mathbf{c}_{IF_i} = e^{j\Delta\phi_{i1}(t_k)} \tag{6.1-22}$$

is the complex signal-reduction function due to phase misalignment between the ith and first signals. Assuming that the ensemble average of the phase difference between any two antennas is independent of which antenna pair is chosen and that the residual phase of each antenna pair is Gaussian distributed with variance $\sigma^2_{\Delta\phi_{i1}}$, then it can be shown that

$$\begin{aligned} \overline{\mathbf{c}_{IFi} \mathbf{c}^*_{IFj}} = C_{ij} &= \mathbf{E}\left\{ e^{j[\Delta\phi_{i1}(t_k) - \Delta\phi_{j1}(t_k)]} \right\} \\ &= \begin{cases} \{ e^{-(1/2)[\sigma^2_{\Delta\phi_{i1}} + \sigma^2_{\Delta\phi_{j1}}]}, & i \neq j, \sigma^2_{\Delta\phi_{11}} \equiv 0 \\ 1 & i = j \end{cases} \end{aligned} \tag{6.1-23}$$

Performing the above averaging operation over $P'_{\mathbf{y}}$, the total signal power is obtained, namely,

$$P_{\mathbf{y}} = P_1\left(\sum_{i=1}^{L}\gamma_i^2 + \sum_{i=1}^{L}\sum_{\substack{j=1\\ i\neq j}}^{L}\gamma_i\gamma_j C_{ij}\right) \tag{6.1-24}$$

Note that in an ideal scenario (i.e., no degradation) with L identical antennas, the signal-reduction functions approach 1 ($C_{ij}=1$ for all i,j) and Eq. (6.1-24) reduces to $P_{\mathbf{y}} = P_1 L^2$. Simultaneously, the noise variance of Eq. (6.1-20) becomes proportional to L and, hence, the SNR increases linearly with L, as expected.

With FSC, only one carrier, one subcarrier, and one symbol-tracking loop are required. The samples of the signal at the output of the integrate-and-dump filter can be expressed as

$$\begin{aligned} v_k &= d_k\sqrt{P_d}C_c C_{sc} C_{sy} + n_k' \\ \sigma_{n'}^2 &= \frac{1}{2T_s}\sum_{i=1}^{L}\beta_i^2 N_{0i} \end{aligned} \tag{6.1-25}$$

where P_d is the combined data power given by $P_{\mathbf{y}}\sin^2\Delta$ and n_k' is Gaussian with variance given by Eq. (6.1-25).

It can be shown that the symbol SNR in terms of $P_{d1} = P_1\sin^2\Delta$ is given by

$$\mathrm{SNR}_{fsc} = \frac{2P_{d1}T_s}{N_{01}}\overline{C_c^2}\,\overline{C_{sc}^2}\,\overline{C_{sy}^2}\left(\frac{\sum_{i=1}^{L}\gamma_i^2 + \sum_{i,j}\sum_{i\neq j}\gamma_i\gamma_j\overline{C}_{ij}}{\Gamma}\right) \tag{6.1-26}$$

where the loop losses are computed using the combined power, whether coming from the carrier or the data. Note that in the ideal case Eq. (6.1-26) reduces to $\mathrm{SNR}_{\mathrm{ideal}} = 2P_{d1}T_s\Gamma/N_{01}$, as expected. The degradation factor for FSC, D_{fsc}, is given as before [Eq. (5.2-3)] by the ratio (in decibels) of the combined symbol SNR to the ideal symbol SNR, i.e.,

$$\begin{aligned} D_{fsc} &= 10\log_{10}\left(\frac{\mathrm{SNR}_{fsc}}{\mathrm{SNR}_{\mathrm{ideal}}}\right) \\ &= 10\log_{10}\left(\overline{C_c^2}\,\overline{C_{sc}^2}\,\overline{C_{sy}^2}\left(\frac{\sum_{i=1}^{L}\gamma_i^2 + \sum_{i,j}\sum_{i\neq j}\gamma_i\gamma_j\overline{C}_{ij}}{\Gamma^2}\right)\right) \end{aligned} \tag{6.1-27}$$

As an example, let $P_i = P_1$, $N_{0i} = N_{01}$, and $\beta_i = 1$ for all antennas; then the signal and noise powers of the real process at the output of the combiner become, respectively,

$$\begin{aligned} P_y &= P_1\left[L + 2(L-1)e^{-\sigma_{\Delta\phi}^2/2} + (L-2)(L-1)e^{-\sigma_{\Delta\phi}^2} \right] \\ \sigma_y^2 &= B N_{01} L \end{aligned} \tag{6.1-28}$$

and the SNR at the combiner output becomes

$$\mathrm{SNR}_{fsc} = \frac{P_y}{\sigma_y^2} = \frac{P_1\left[L + 2(L-1)e^{-\sigma_{\Delta\phi}^2/2} + (L-2)(L-1)e^{-\sigma_{\Delta\phi}^2} \right]}{B N_{01} L} \tag{6.1-29}$$

With perfect alignment (i.e., $\sigma_{\Delta\phi}^2 \to 0$), the SNR_z reduces to

$$\mathrm{SNR}_{\mathrm{ideal}} = \frac{P_1 L}{N_{01} B} \tag{6.1-30}$$

as expected and, hence, the combining degradation for the FSC scheme is given by

$$D_{fsc} = 10\log_{10}\left[\frac{L + 2(L-1)e^{-\sigma_{\Delta\phi}^2/2} + (L-2)(L-1)e^{-\sigma_{\Delta\phi}^2}}{L^2} \right] \tag{6.1-31}$$

Note that D_{fsc} ideally approaches zero. For the case of a single antenna (i.e., no arraying), D_{fsc} measures the degradation due to imperfect synchronization. Figures 6-5 and 6-6 depict the degradation of FSC, D_{fsc}, for the array of two high-efficiency (HEF) antennas and one standard (STD) 34-m antenna as a function of P/N_0 of the master antenna (Fig. 6-5) and of modulation index Δ (Fig. 6-6). Also depicted is the degradation due to any single synchronization step (such as carrier, subcarrier, or symbol synchronization), obtained by setting the degradation due to the other steps to zero. An "x" has been placed in the figure to indicate the point at which carrier-loop SNR dips below 8 dB and significant cycle slipping occurs. Because with FSC the carrier loop tracks the combined signal, there is less degradation than when several carrier loops track individual signals, as in the case of symbol-stream combining or baseband combining (discussed in Sections 6.3 and 6.4).

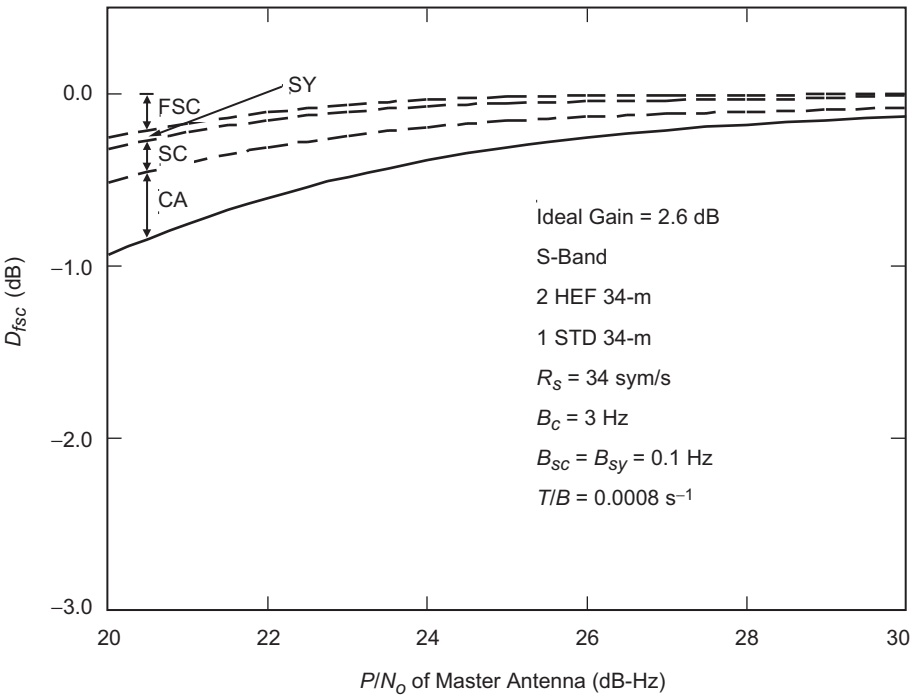

Fig. 6-5. The D_{fsc} versus P_1/N_{01} for a modulation index of 65.9 deg.

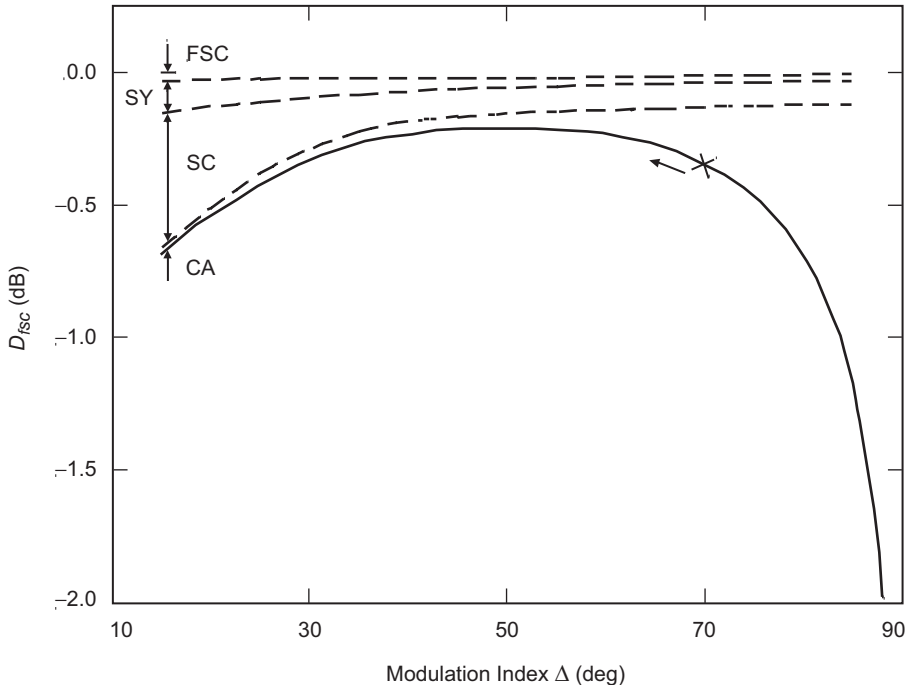

Fig. 6-6. The D_{fsc} versus modulation index for P_1/N_{01} = 25 dB-Hz.

6.2 Complex-Symbol Combining (CSC)

As depicted in Figs. 6-7 and 6-8, signals from multiple antennas in CSC are open-loop downconverted to baseband; partially demodulated using multiple subcarrier loops, multiple symbol loops, and multiple matched filters; and then combined and demodulated using a single baseband carrier loop. The advantage of CSC is that the symbol-combining loss is negligible and is performed in the data-rate bandwidth. Moreover, antennas that are continents apart can transmit their symbols in real or nonreal time to a central location, where the symbol-stream combiner outputs the final symbols. That, however, requires that each

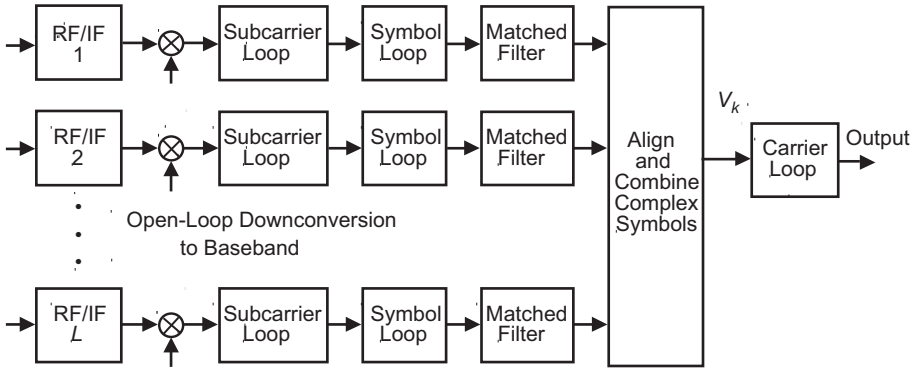

Fig. 6-7. The complex-symbol combining (CSC) algorithm for an *L*-antenna array.

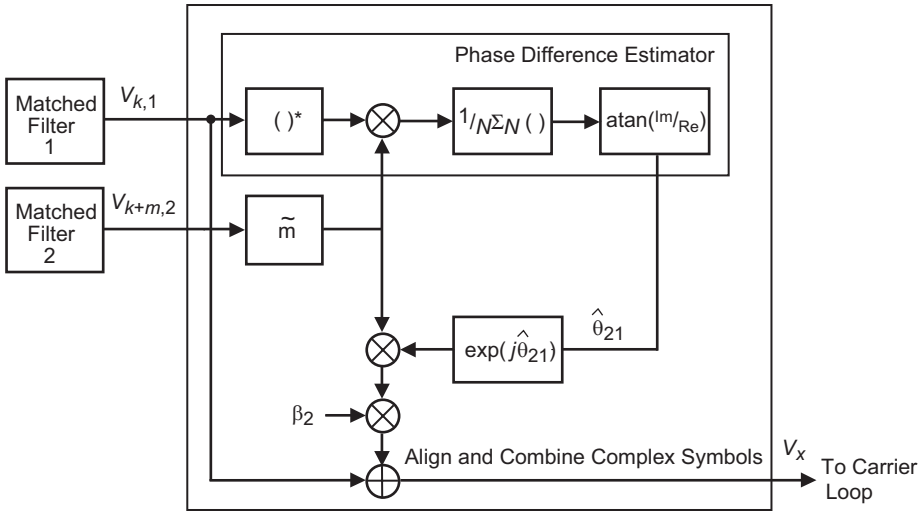

Fig. 6-8. CSC align and combine for a two-antenna array.

antenna is able to lock on the signal individually. The disadvantage of CSC is that L subcarrier and L symbol-tracking devices are needed, and each suffers some degradation.

The subcarrier and symbol loops used for CSC can be the same as those used in FSC or they can be slightly modified versions that take advantage of both the in-phase (I) and quadrature-phase (Q) components of the signal. CSC implementations with the same loops as in the FSC would use either the I- or Q-component of the baseband signal. In either case, the loop SNRs of the subcarrier and symbol loops need to be recomputed since the loop input can no longer be assumed to have carrier lock. Let ρ_{sci}^{I} denote the loop SNR of the ith subcarrier loop when either the I- or Q-arm is used (i.e., the unmodified loop), and let ρ_{sci}^{IQ} denote the subcarrier-loop SNR when both the I- and Q-arms are used (i.e., the modified loop). Similarly, define ρ_{syi}^{I} and ρ_{syi}^{IQ} for the ith symbol loop; then, from Appendix F, we have

$$\begin{aligned}
\rho_{sci}^{I} &= \left(\frac{2}{\pi}\right)^2 \frac{P_{di}/N_{0i}}{2B_{sci}w_{sci}}\left(1+\frac{1}{P_{di}T_s/N_{0i}}\right)^{-1} \\
\rho_{sci}^{IQ} &= \left(\frac{2}{\pi}\right)^2 \frac{P_{di}/N_{0i}}{B_{sci}w_{sci}}\left(1+\frac{1}{P_{di}T_s/N_{0i}}\right)^{-1} \\
\rho_{syi}^{I} &= \frac{1}{2\pi^2}\frac{P_{di}/N_{0i}}{B_{syi}w_{syi}}\mathrm{L}_I \\
\rho_{syi}^{IQ} &= \frac{1}{2\pi^2}\frac{P_{di}/N_{0i}}{B_{syi}w_{syi}}\mathrm{L}_{IQ}
\end{aligned} \tag{6.2-1}$$

where $B_{sci}w_{sci}$ and $B_{syi}w_{syi}$ are the window-loop bandwidth products of the ith subcarrier and symbol loops, respectively. Squaring losses L_I for the unmodified loop and L_{IQ} for the modified loop are defined in Appendix F. For the Galileo S-Band Mission (see parameters specified in the numerical examples of Chapter 7), it is shown in Appendix F that using the unmodified subcarrier and symbol loop reduces the loop SNR by 6 dB as compared with the carrier-locked case, and that utilizing both the I- and Q-arms recovers 3 of the 6 dB. Consequently, since the modified subcarrier and symbol loops result in an improved performance, they will be used in this section when comparing CSC with FSC. (The actual operating bandwidths for the modified and unmodified subcarrier and symbol loops also are investigated in Appendix F.)

Referring to Fig. 6-7, the combining gain is maximized by aligning the baseband signals in time and phase prior to combining. The alignment algorithm for an array of two antennas is shown in Fig. 6-8. Here signal 1 is

assumed to be delayed by m symbols with respect to signal 2. Therefore, the signals are time aligned by delaying signal 2 by $\tilde{m}$ symbols, where $\tilde{m}$ is an estimate of m. As in FSC, we assume perfect time alignment so that $\tilde{m} = m$. After time alignment, the phase of signal 2 with respect to signal 1 is assumed to be θ_{21} rad. Hence, the signals are phase aligned by rotating signal 2 by the phase estimator output $\hat{\theta}_{21}$.

The analysis of CSC degradation begins with the expression for the output of the matched filter in Fig. 6-7. Note that there are actually *2L* matched filters per *L* antennas because, after subcarrier demodulation, a real symbol stream is modulated by I- and Q-baseband tones. Using complex notation, the matched-filter output stream corresponding to the *k*th symbol and the *i*th antenna, conditioned on $\phi_{sc\,i}$ and $\phi_{sy\,i}$, can be written as

$$\mathbf{v}_{k\,i} = \sqrt{P_i} C_{sci} C_{syi} d_k e^{j[\Delta\omega_c t_k + \theta_{i1}]} + \mathbf{n}_{k\,i} \tag{6.2-2}$$

where the noise $\mathbf{n}_{k\,i}$ is a complex Gaussian random variable with variance N_{0i}/T_s. The subcarrier- and symbol-reduction functions, C_{sci} and C_{syi}, are given by Eq. (5.2-9) after replacing ϕ_{sc} by $\phi_{sc\,i}$ and ϕ_{sy} by $\phi_{sy\,i}$. The baseband carrier frequency $\Delta\omega_c/(2\pi)$ is equal to the difference between the predicted and actual IF carrier frequencies and is assumed to be much less than the symbol rate, i.e., $\Delta f_c << 1/T_s$. The degradation at the output of the matched filter when the carrier is open-loop downconverted is approximately given as

$$D_{\Delta f_c} = \left(\frac{\sin(\Delta f_c T_s / 2)}{\Delta f_c T_s / 2} \right)^2 \tag{6.2-3}$$

Figure 6-9 illustrates the matched-filter degradation as a function of $\Delta f_c T_s$, and it is clear that the degradation is less than 0.0129 dB when $\Delta f_c T_s < 0.03$.

The combined signal after phase compensation, $\mathbf{v}_k$ in Fig. 6-7, is given as

$$\mathbf{v}_k = \sum_{i=1}^{L} \beta_i \mathbf{v}_{k\,i} e^{-j\hat{\theta}_{i1}} \tag{6.2-4}$$

where $\mathbf{v}_{k\,i}$ is given in Eq. (6.2-2) and $\hat{\theta}_{i1}$ is an estimate of θ_{i1}.

After substituting Eq. (6.2-2), the combined signal can be rewritten as follows (see Appendix G):

$$\mathbf{v}_k = \sqrt{P'} d_k e^{j[\Delta\omega_c t_k + \theta_v]} + \mathbf{n}_k \tag{6.2-5}$$

where the variance of the combined complex noise is given as [3]

$$\sigma^2_{\mathbf{n}_k} = \frac{N_{01}}{T_s} \sum_{i=1}^{L} \gamma_i = \frac{N_{01}}{T_s} \Gamma \tag{6.2-6}$$

The conditional combined signal power, P', is given as

$$P' = P_1 \sum_{i=1}^{L} \sum_{j=1}^{L} \gamma_i \gamma_j C_{sci} C_{scj} C_{syi} C_{syj} C_{ij} \tag{6.2-7}$$

where $C_{ij} = e^{j[\Delta\phi_{i1} - \Delta\phi_{j1}]}$ [as in Eq. (6.1-23)]. The signal $\mathbf{v}_k$ then is demodulated using a baseband Costas loop with output equal to $e^{-j(\Delta\omega_c t_k + \hat{\theta}_v)}$, where $\hat{\theta}_{\mathbf{v}}$ is an estimate of $\theta_{\mathbf{v}}$. The demodulator output is a real combined symbol stream and can be represented as

$$v_k = \sqrt{P'} C_c d_k + n_k \tag{6.2-8}$$

where C_c and P' are respectively given by Eqs. (5.2-9) and (6.2-7). The noise n_k is a real Gaussian random variable with variance $\sigma_n^2 = \sigma_{\mathbf{n}}^2 / 2$, where $\sigma_{\mathbf{n}}^2$ is given by Eq. (6.2-6). The SNR conditioned on $\phi_c, \phi_{sci}, \phi_{syi}, \Delta\phi_{i1}$, denoted SNR'_{csc}, is defined as the square of the conditional mean of v_k divided by the conditional variance of v_k, i.e.,

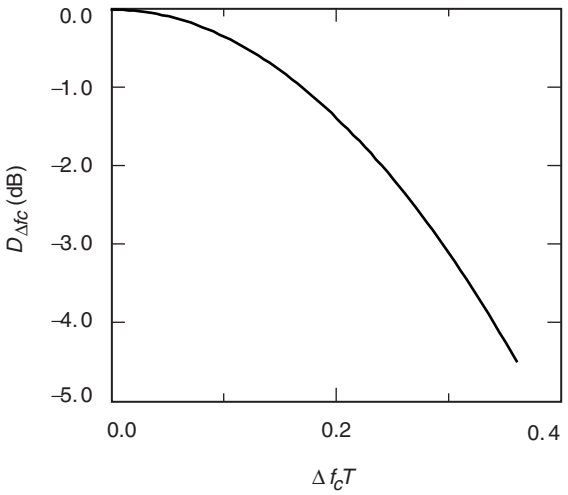

Fig. 6-9. Degradation at the matched-filter output versus the carrier frequency error–symbol time product.

$$\mathrm{SNR}'_{csc} = \frac{2P_1T_s}{N_{01}} C_c^2 \frac{\sum_{i=1}^{L}\sum_{j=1}^{L} \gamma_i\gamma_j C_{sci}C_{scj}C_{syi}C_{syj}C_{ij}}{\Gamma} \tag{6.2-9}$$

6.2.1 Telemetry Performance

The degradation is found, as before, by dividing the unconditional CSC SNR, which includes the effects of synchronization and alignment errors, by the ideal SNR. The unconditional SNR, denoted SNR_{csc}, is computed by taking the statistical expectation of SNR'_{csc} with respect to $\phi_c, \phi_{sci}, \phi_{syi,} \Delta\phi_{i1}$. The phase probability densities are assumed to be the same as before. In addition, ϕ_{sci} and ϕs_{scj} are assumed to be independent when $i \neq j$, and the same is true for ϕ_{syi} and ϕ_{syj}. Consequently,

$$\mathrm{SNR}_{csc} = \frac{2P_1T_s}{N_{01}} \overline{C_c^2} \frac{\sum_{i=1}^{L} \gamma_i^2 \overline{C_{sci}^2}\,\overline{C_{syi}^2} + \sum_{i=1}^{L}\sum_{j=1}^{L} \gamma_i\gamma_j \overline{C}_{sci}\overline{C}_{scj}\overline{C}_{syi}\overline{C}_{syj}\overline{C}_{ij}}{\Gamma} \tag{6.2-10}$$

where the average signal-reduction function due to phase misalignment between baseband signals i and j, denoted $\overline{C}_{ij}$, is given by Eq. (6.1-23) with $\sigma^2_{\Delta\phi i1} = 1/\mathrm{SNR}_{csci1}$. The CSC correlator SNR, or $\mathrm{SNR}_{\mathrm{csc}i1}$, is shown in Appendix G to be

$$\mathrm{SNR}_{csci1} = \frac{P_1}{N_{01}} \frac{T\,\overline{C_{sci}^2}\,\overline{C_{sc1}^2}\,\overline{C_{syi}^2}\,\overline{C_{sy1}^2}}{\overline{C_{sci}^2}\,\overline{C_{syi}^2} + \overline{C_{sc1}^2}\,\overline{C_{sy1}^2}\,\dfrac{1}{\gamma_i} + \dfrac{N_{0i}}{PT_s}} \tag{6.2-11}$$

where T is the averaging time of the correlator and T_s is the symbol period. The loop-reduction functions $\overline{C_{sci}}, \overline{C_{sci}^2}, \overline{C_{syi}}$, and $\overline{C_{syi}^2}$ for the ith subcarrier and symbol loops are given by Eq. (5.2-9), where the loop SNRs are given by Eqs. (E-7) and (E-14).

The carrier-loop loss $\overline{C_c^2}$ also is given by Eq. (5.2-9) with the loop SNR ρ_c in that equation computed using the average combined power P'/N_{0eff}, found by averaging Eq. (6.2-7) over all phases and dividing by the effective noise level, $N_{0eff} = T_s\sigma_{\mathbf{n}}^2$. Ideally, with no phase errors, $\overline{C_c^2} = \overline{C_{sc}^2} = \overline{C_{sy}^2} = \overline{C_{sc}} = \overline{C_{sy}} = \overline{C_{ij}} = 1$ and Eq. (6.2-10) reduces to $2P_1T_s\Gamma/N_{01}$, as expected. The degradation will be

$$D_{\text{csc}} = 10\log\left[\overline{C_c^2}\,\frac{\sum_{i=1}^{L}\gamma_i^2\overline{C_{sc\,i}^2}\,\overline{C_{sy\,i}^2} + \sum_{i=1}^{L}\sum_{\substack{j=1\\ i\neq j}}^{L}\gamma_i\gamma_j\overline{C}_{sc\,i}\overline{C}_{sc\,j}\overline{C}_{sy\,i}\overline{C}_{sy\,j}\overline{C}_{ij}}{\Gamma^2}\right] \quad (6.2\text{-}12)$$

Several examples of this scheme for the Galileo Mission are given in the numerical examples of Chapter 7.

6.3 Symbol-Stream Combining (SSC)

SSC involves the arraying of real symbols, as opposed to complex symbols. As with CSC, the advantage of SSC is that the combining loss is negligible [4] and is performed in the data-rate bandwidth. Moreover, antennas that are continents apart can transmit their symbols in real or nonreal time to a central location, where the symbol-stream combiner outputs the final symbols. However, that requires each antenna to be able to lock on the signal individually. The disadvantage of SSC is that L carrier, L subcarrier, and L symbol-tracking devices are needed, and each suffers some degradation. For moderate-to-high modulation indices, the carrier degradation can be reduced by employing sideband aiding at each antenna.

As depicted in Fig. 6-10, each antenna tracks the carrier and the subcarrier and performs symbol synchronization individually. The symbols at the output of each receiver then are combined with the appropriate weights to form the final detected symbols. The samples of the signal at the output of the symbol-stream combiner are

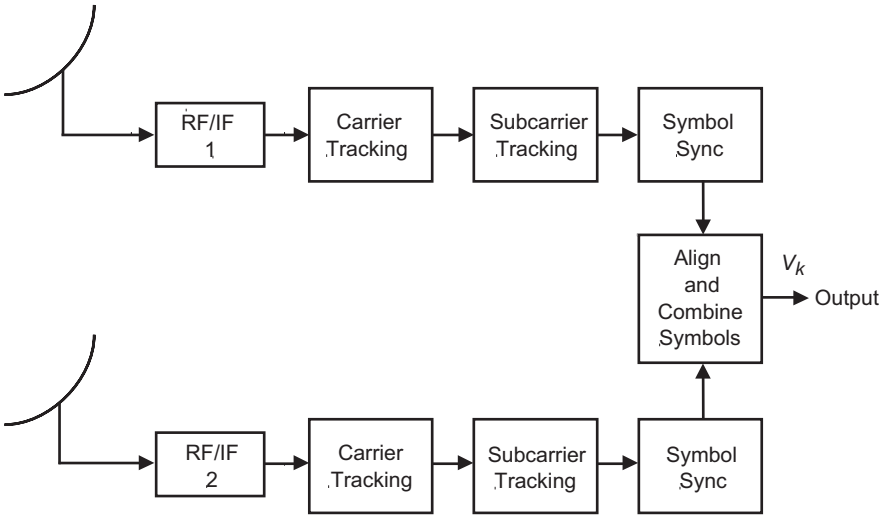

Fig. 6-10. Symbol-stream combining (SSC).

$$v_k = d_k \sum_{i=1}^{L} \beta_i \sqrt{P_{di}} C_{ci} C_{sci} C_{syi} + n'_k \tag{6.3-1}$$

where the β_i are weighing factors given by Eq. (6.1-19), $P_{di} = P_i \sin^2 \Delta$ is the received data power at antenna i (P_i is the total received power), and C_{ci}, C_{sci}, and C_{syi} are the degradation functions at the ith antenna, as defined in Eq. (5.2-9). There is negligible loss when combining the symbols (<0.05 dB), and, assuming that each receiver chain has a one-sided noise power spectral density level N_{0i}, it is straightforward to show [5] that the variance of n'_k is given by

$$\sigma^2_{n'_k} = \frac{1}{2T_s} \sum_{i=1}^{L} \beta_i^2 N_{0i} \tag{6.3-2}$$

The conditional symbol SNR (assuming that the various phase errors are known) at the output of the combiner is

$$\mathrm{SNR}'_{ssc} = \frac{\left[\overline{v_k}\right]^2}{\sigma^2_{n'}} \tag{6.3-3}$$

where $\bar{v}_k$ is the mean of v_k conditioned on $\phi_{ci}, \phi_{sci}, \phi_{syi}$ for i=1,...,L. Using Eqs. (6.1-10), (6.3-1), and (6.3-2) in Eq. (6.3-3), we get

$$\mathrm{SNR}'_{ssc} = \frac{2P_{d1}T_s}{N_{01}} \frac{\left(\sum_{i=1}^{L} \gamma_i C_{ci} C_{sci} C_{syi} \right)^2}{\Gamma} \tag{6.3-4}$$

Note that, in the absence of any degradation, the conditional SNR simplifies to

$$\mathrm{SNR}_{\mathrm{ideal}} = \frac{2P_{d1}T_s}{N_{01}} \sum_{i=1}^{L} \gamma_i = \frac{2P_{d1}T_s}{N_{01}} \Gamma \tag{6.3-5}$$

with Γ being the ideal gain factor obtained at antenna 1, which again for convenience is denoted as the master antenna. For L identical antennas with equal noise temperatures, we have $\gamma_i = \gamma_1 = 1$ for i = 2...L, and the ideal SNR reduces to $2LP_{d1}T_s / N_{01}$, as expected. The actual SNR at the output of the symbol combiner is obtained by averaging the conditional SNR over the unknown phase errors, which are embedded in the constants $C_{ci}C_{sci}C_{syi}$ defined in Eq. (5.1-5), i.e.,

$$\mathrm{SNR}_{ssc} = \frac{2P_{d1}T_s}{N_{01}}\left(\frac{\sum_{i=1}^{L}\gamma_i^2\overline{C_{ci}^2}\,\overline{C_{sci}^2}\,\overline{C_{syi}^2} + \sum_{i=1}^{L}\sum_{\substack{j=1\\ i\neq j}}^{L}\gamma_i\gamma_j\,\overline{C}_{ci}\overline{C}_{sci}\overline{C}_{syi}\,\overline{C}_{cj}\overline{C}_{scj}\overline{C}_{syj}}{\Gamma}\right) \tag{6.3-6}$$

Because the noise processes make all the phase errors mutually independent, the computation of the unconditional SNR in Eq. (6.3-6) reduces to the computation of the first two moments of the various C_{ci}, C_{sci}, and C_{syi} given in Eq. (5.2-9). Finally, we define the SNR degradation factor D_{ssc} (in decibels) for symbol-stream combining as

$$\begin{aligned} D_{ssc} &= 10\log_{10}\left(\frac{\mathrm{SNR}_{ssc}}{\mathrm{SNR}_{ideal}}\right) \\ &= 10\log_{10}\left(\frac{\sum_{i=1}^{L}\gamma_i^2\overline{C_{ci}^2}\,\overline{C_{sci}^2}\,\overline{C_{syi}^2} + \sum_{i=1}^{L}\sum_{\substack{j=1\\ i\neq j}}^{L}\gamma_i\gamma_j\,\overline{C}_{ci}\overline{C}_{sci}\overline{C}_{syi}\,\overline{C}_{cj}\overline{C}_{scj}\overline{C}_{syj}}{\Gamma^2}\right) \end{aligned} \tag{6.3-7}$$

Figures 6-11 and 6-12 depict D_{ssc} for an array of the same three antennas as were used in the FSC example as a function of P/N_0 of the master antenna (Fig. 6-11) and of the modulation index (Fig. 6-12). Also depicted is the degradation due to any single synchronization step (such as carrier, subcarrier, or symbol) obtained by setting the contribution due to the other steps to zero.

6.4 Baseband Combining (BC)

In baseband combining, each antenna locks on the carrier signal, as depicted in Fig. 6-13. The baseband signals, consisting of data on a subcarrier, are digitized, aligned in time, and combined, and the symbols are demodulated. The combined digital symbols can be modeled as

$$v_k = d_k C_{sc} C_{sy} \sum_{i=1}^{L} \beta_i \sqrt{P_{di}}\, C_{ci} C_{bbi} + n_k' \tag{6.4-1}$$

where $C_{bbi} = (1 - 2m\,|\,\tau_i\,|)$ is the signal-reduction function for the baseband combiner, m is the ratio of the subcarrier frequency over the symbol rate, and τ_i is the delay error of the ith telemetry time-aligning loop ($\tau_1 = 0$) [6]. For the combined signal, only one subcarrier and one symbol-tracking loop are

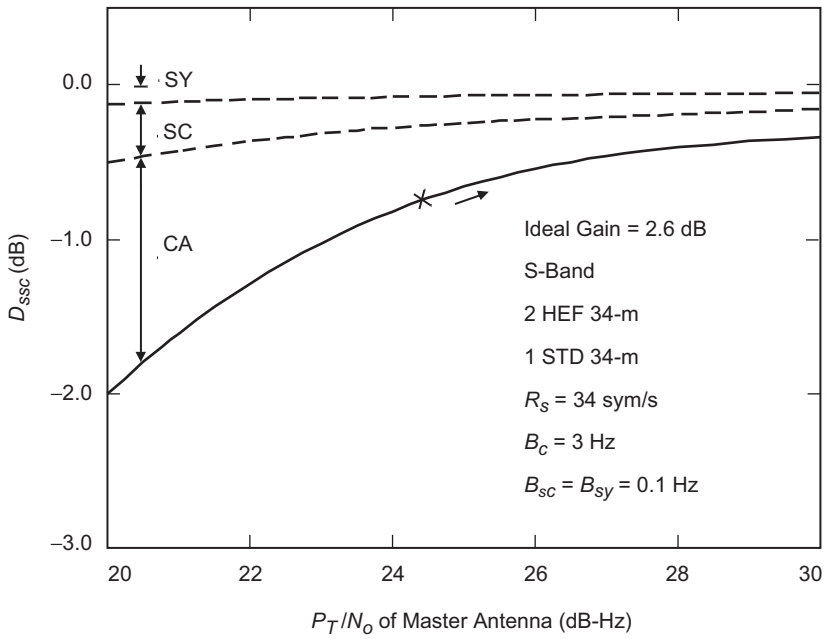

Fig. 6-11. The degradation of SSC versus P_1/N_{01} for a modulation index of 65.9 deg.

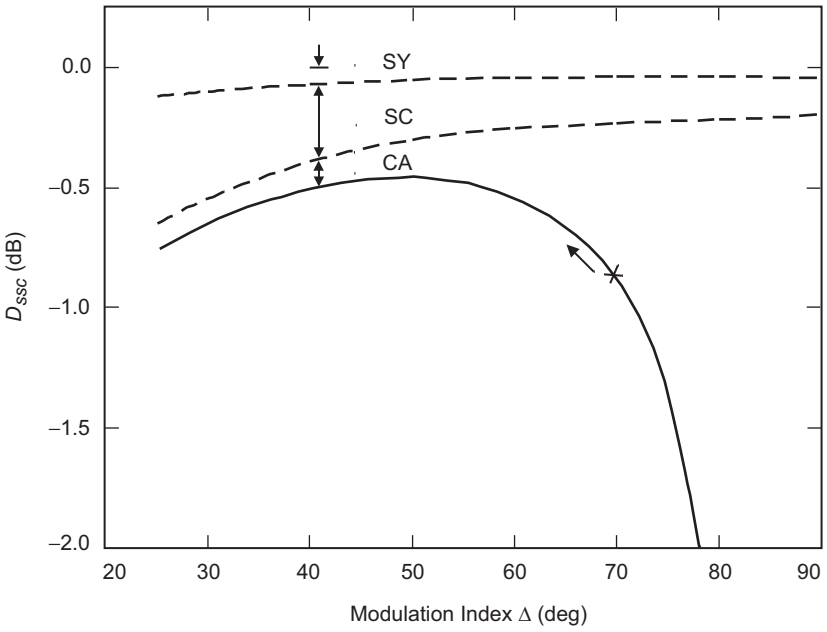

Fig. 6-12. The degradation of SSC versus modulation index for a P_1/N_{01} of 25 dB-Hz.

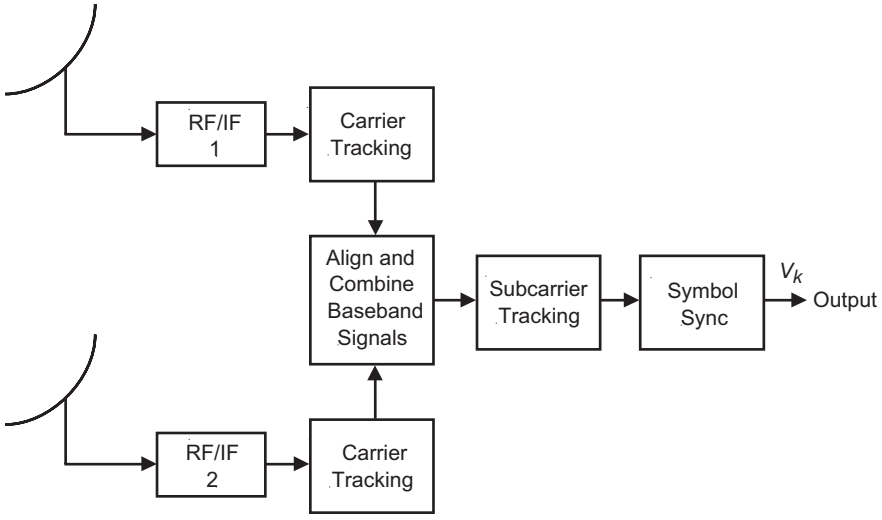

Fig. 6-13. Baseband combining (BC).

employed and, hence, no subscripts are needed for the random variables ϕ_{sc} and ϕ_{sy}. The variance of v_k due to thermal noise still is given by Eq. (6.3-2). Again, as with the SSC scheme, the conditional SNR at the output of the matched filter is given by

$$\mathrm{SNR}'_{bc} = \frac{\left(\overline{v_k \mid \phi_c, \phi_{sc}, \phi_{sy}, \tau_i}\right)^2}{N_{01}} = \frac{2P_{d1}T_s}{N_{01}} C_{sc}^2 C_{sy}^2 \frac{\left(\sum_{i=1}^{L} \gamma_i C_{c\,i} C_{bb\,i}\right)^2}{\Gamma} \tag{6.4-2}$$

In order to compute the unconditional SNR, we have to average Eq. (6.4-2) over all the phase- and delay-error processes in the corresponding tracking loops, resulting in

$$\mathrm{SNR}_{bc} = \frac{2P_{d1}T_s}{N_{01}} \overline{C_{sc}^2}\,\overline{C_{sy}^2} \left(\frac{\sum_{i=1}^{L} \gamma_i^2 \overline{C_{c\,i}^2}\,\overline{C_{bb\,i}^2} + \sum_{i,j} \sum_{i \neq j} \gamma_i \gamma_j \overline{C}_{c\,i} \overline{C}_{c\,j} \overline{C}_{bb\,i} \overline{C}_{bb\,j}}{\Gamma} \right) \tag{6.4-3}$$

The signal-reduction function for the time alignment of baseband signals, $C_{bb\,i}$, has the following first two moments:

$$\begin{aligned}\overline{C}_{bbi} &= \left(1 - 2m\sqrt{\frac{2}{\pi}}\sigma_{\tau i}\right) \\ \overline{C^2_{bbi}} &= \left(1 - 4m\sqrt{\frac{2}{\pi}}\sigma_{\tau i} + 4m^2\sigma^2_{\tau i}\right)\end{aligned} \tag{6.4-4}$$

where $\sigma^2_{\tau i}$ denotes the variance of the ith time-aligning loop and is computed to be [6]

$$\sigma^2_{\tau i} = \frac{B_{\tau i}}{B_n 32\, m^2}\left(\frac{1}{\left[erf\left(\sqrt{P_{d1}\sigma^2_1}\right)erf\left(\sqrt{P_{di}\sigma^2_i}\right)\right]^2} - 1\right), \quad i = 2,...,L \tag{6.4-5}$$

In the above equation, $B_{\tau i}$ denotes the bandwidth of the time-aligning loops, B_n the noise bandwidth at the input to the digitizer (assumed to be the same in all channels), and $\sigma^2_i = N_{0i}B_n$ (note that $\overline{C}_{bbi} = 1$ and $\overline{C^2_{bbi}} = 1$). The equations for the moments of C_{sc} and C_{sy} are those given by Eq. (5.2-9) with the variances computed using the combined P_d / N_0. Note that under ideal conditions (i.e., no phase or delay errors in the tracking loops), all C's are 1, and the SNR reduces to

$$\text{SNR}_{\text{ideal}} = \frac{2P_{d1}T_s}{N_{01}}\Gamma \tag{6.4-6}$$

as in the symbol-stream combining case [Eq. (6.3-5)]. As expected, BC has the same SNR performance as other schemes under ideal conditions. Once the unconditional SNR is computed for the BC scheme using Eq. (6.4-3), the degradation factor is obtained as before, namely,

$$\begin{aligned}D_{bc} &= 10\log_{10}\left(\frac{\text{SNR}_{\text{bc}}}{\text{SNR}_{\text{ideal}}}\right) \\ &= 10\log_{10}\left(\frac{\sum_{i=1}^{L}\gamma_i^2\overline{C^2_{ci}}\,\overline{C^2_{bbi}} + \sum_{i,j}\sum_{i\neq j}\gamma_i\gamma_j\overline{C}_{ci}\overline{C}_{cj}\overline{C}_{bbi}\overline{C}_{bbj}}{\overline{C^2_{sc}}\,\overline{C^2_{sy}}\,\Gamma^2}\right)\end{aligned} \tag{6.4-7}$$

Figures 6-14 and 6-15 depict the degradation due to baseband combining, D_{bc}, as a function of both P_1 / N_{01} (Fig. 6-14) and Δ (Fig. 6-15), assuming the same array as in the FSC case. Note from Fig. 6-14 that the subcarrier and

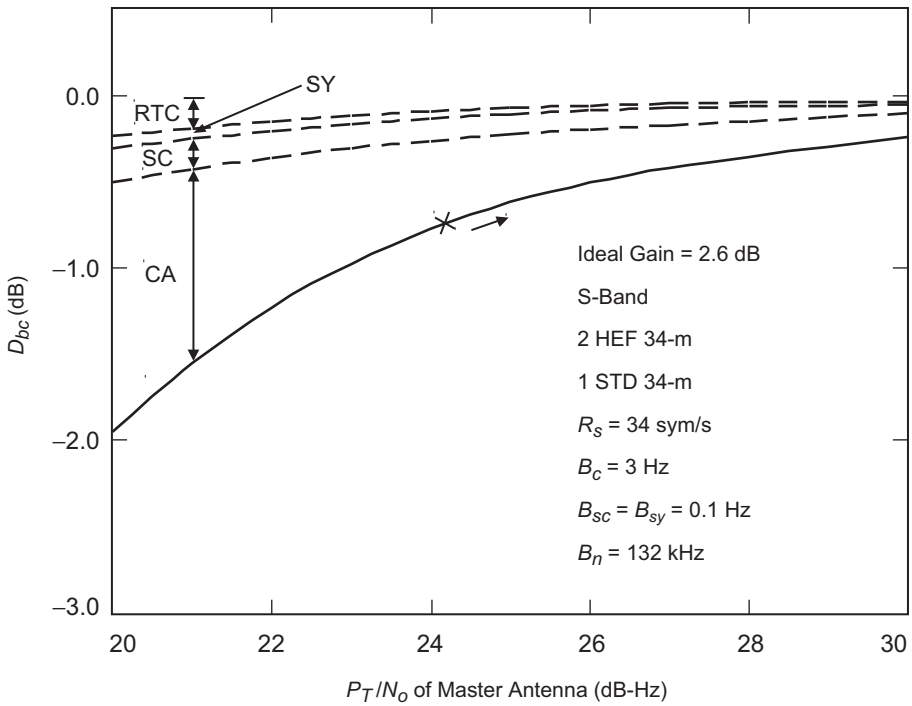

Fig. 6-14. The degradation of BC versus P_1/N_{01} for a modulation index of 65.9 deg.

symbol degradations are less than their counterparts in SSC (Fig. 6-11) because these loops track the combined signal.

6.5 Carrier Arraying (CA)

In carrier arraying, several carrier-tracking loops are coupled in order to enhance the received carrier signal-to-noise ratio and, hence, decrease the telemetry (radio) loss due to imperfect carrier synchronization. The coupling can be performed using phase-locked loops (PLLs) for residual carriers or Costas loops for suppressed BPSK carriers. Only the PLL case is considered here to illustrate the idea of carrier arraying. A general block diagram is shown in Fig. 6-16, where two carrier loops share information to jointly improve their performance, as opposed to tracking individually. Carrier arraying by itself does not combine the data and thus needs to operate with baseband combining or symbol-stream combining to array the telemetry. This is shown in Fig. 6-16, where baseband combining is employed to array the data spectrums.

There are basically two scenarios in which one would employ carrier arraying. In the first scenario, a large antenna locks on the signal by itself and

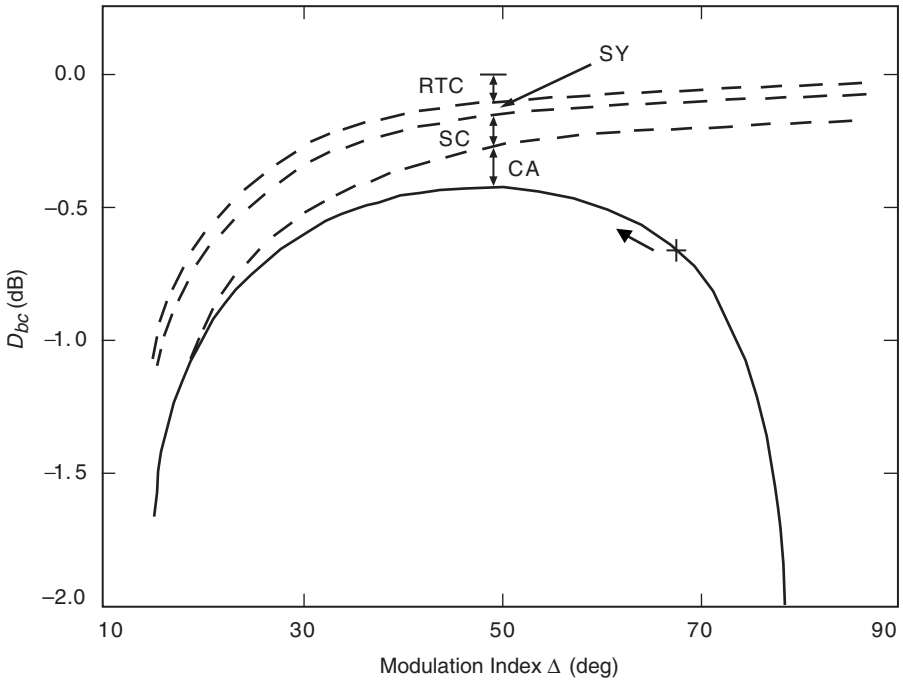

Fig. 6-15. The degradation of BC versus modulation index for a P_1/N_{01} of 25 dB-Hz.

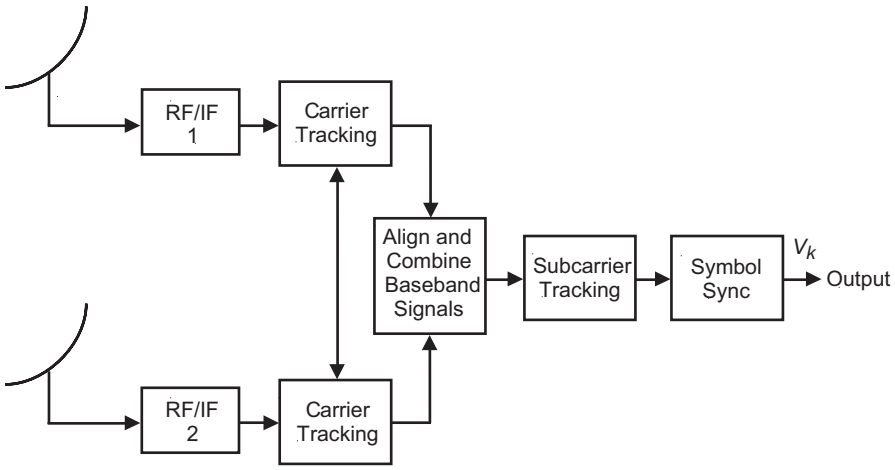

Fig. 6-16. Carrier arraying with baseband combining (CA/BC).

then helps a smaller antenna track. In this case, the signal might experience dynamics requiring a large loop bandwidth and, hence, the signal would have to be strong enough to enable the carrier loop to operate with the large bandwidth. A large antenna with a strong signal first is used to track the signal and then the dynamics of the signal are estimated and removed from the weaker signal to enable the other carrier loop to operate with a smaller bandwidth and, hence, a higher loop SNR. In the second scenario, the signal is too weak to be tracked by any single antenna but can be tracked jointly by two or more antennas. The combining methods used in the latter case are similar to those employed in FSC when aligning the phases of pure tones (hence, requiring a smaller correlator bandwidth). In either scenario, carrier arraying can be implemented in one of two ways—at baseband or at an intermediate frequency (IF).

6.5.1 Baseband Carrier-Arraying Scheme

Baseband carrier arraying is illustrated in Fig. 6-17, where the error signals at the output of the phase detectors are combined at baseband. This scheme is analyzed in [7], where it is shown that the variance of the phase-jitter process in the master PLL is given by

$$\sigma_{c1}^2 = \frac{1}{2\pi j}\oint\left[\frac{H_1(z)}{1+\sum_{i=2}^{L}\gamma_i H_1(z)[1-H_i(z)]}\right]^2 \frac{dz}{z}\frac{N_{01}}{2T_{c1}P_{c1}} + \sum_{i=2}^{L}\gamma_i^2\frac{1}{2\pi j}\oint\left[\frac{H_1(z)[1-H_i(z)]}{1+\sum_{i=2}^{L}\gamma_i H_1(z)[1-H_i(z)]}\right]^2 \frac{dz}{z}\frac{N_{0i}}{2T_{ci}P_{ci}} \tag{6.5-1}$$

where $H_i(z)$ is the closed-loop transfer function of the ith loop and T_{ci} is the loop update time. The above integral is difficult to evaluate in general. However, when $B_{ci} << B_{c1}$ for $i = 2,...,L,$ which is the preferred mode of operation, the above integral can be approximated by

$$\sigma_{c1}^2 = \frac{B_{ci}\sum_{i=1}^{L}\beta_i^2 N_{0i}}{P_{c1}\Gamma^2} \tag{6.5-2}$$

which assumes ideal performance. In this case, the master-loop SNR becomes

$$\rho_{c1} = \frac{P_{c1}}{B_{c1}N_{01}}\Gamma \tag{6.5-3}$$

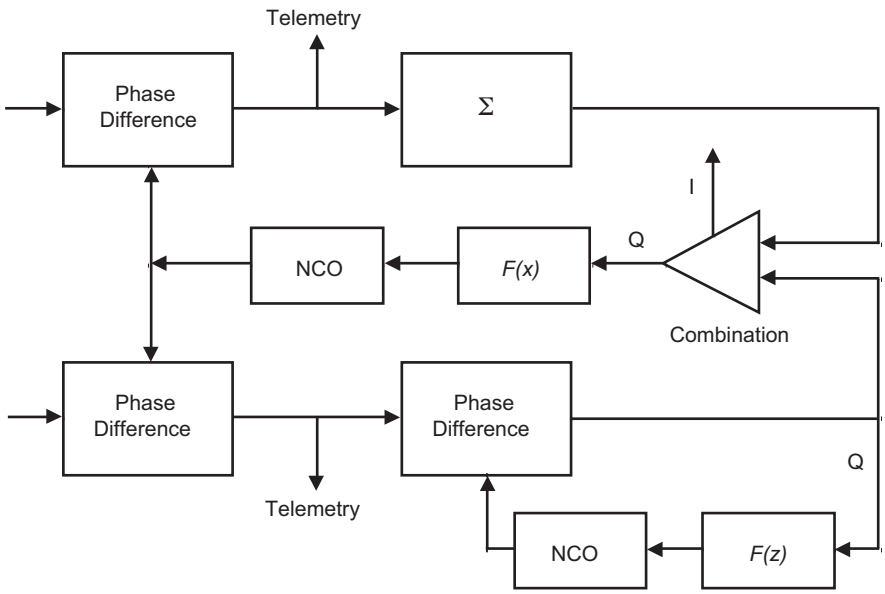

Fig. 6-17. A baseband implementation of carrier arraying.

assuming identical noise spectral densities. The actual variance typically will be larger and requires the evaluation of Eq. (6.5-1), which depends on the actual loop filters implemented.

6.5.2 IF Carrier-Arraying Scheme

One form of IF carrier arraying is depicted in Fig. 6-18 and is conceptually the same as full-spectrum combining. In this case, the carrier power, P_{ci}, is substituted for the total power, P_i. So, all equations and results derived for the FSC scheme regarding the combining loss can be automatically applied to the IF carrier-arraying scheme. Phase estimation in this case can be performed by downconverting the received IFs to baseband using a precomputed model of the received Doppler and Doppler rate. The correlation can be computed at baseband using very small bandwidths B and, hence, requiring short integration times T. From Eq. (6.1-8), the variance of the ith carrier correlator is

$$\sigma_{ci}^2 = B(N_{01}P_{ci} + N_{0i}P_{c1} + N_{01}N_{0i}B) \approx N_{01}N_{0i}B^2 \tag{6.5-4}$$

while the correlator's SNR is

$$\mathrm{SNR}_c \cong \frac{P_{c1}}{N_{01}}\frac{P_{ci}}{N_{0i}}\frac{2T}{B} \tag{6.5-5}$$

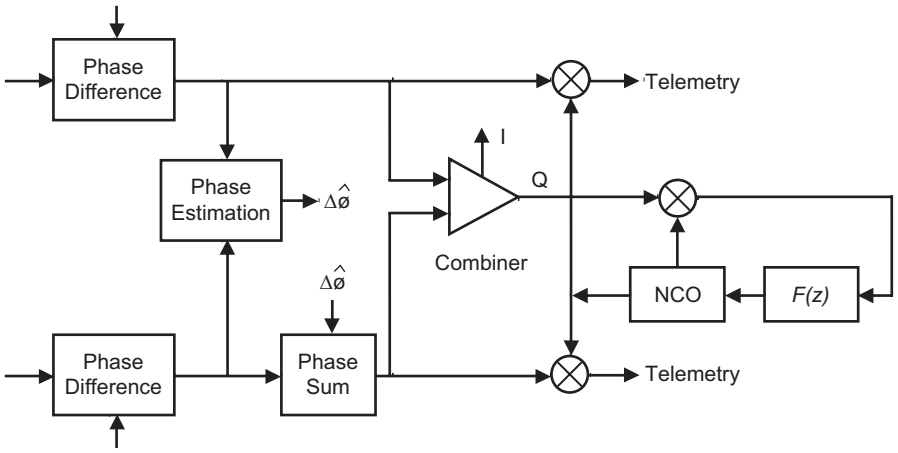

Fig. 6-18. An IF implementation of carrier arraying.

Note that, for IF carrier arraying, the bandwidth B is much narrower than that used in FSC since the data spectrum is not employed. The signal combiner performs the weighted sum of carrier signals $\mathbf{c}_i(t)$, giving the complex combined carrier signal

$$\mathbf{c}(t) = \sum_{i=1}^{L} \beta_i \left[\sqrt{P_{ci}}\, e^{j[\omega_{Ii} t + \theta_1(t) + \Delta\phi_{ci}(t)]} \right] + \mathbf{n}_i(t)\, e^{j[\omega_{Ii} t + \theta_1(t) + \Delta\phi_{ci}(t)]} \tag{6.5-6}$$

Following Eqs. (6.1-21) through (6.1-24), the average carrier power and the variance of the combined complex carrier signal $\mathbf{c}(t)$ are, respectively,

$$\begin{aligned} P_{\mathbf{c}} &= \sum_{i=1}^{L} \beta_i^2 P_{ci} + \sum_{i=1}^{L} \sum_{\substack{j=1 \\ i \neq j}}^{L} \beta_i \beta_j \sqrt{P_{ci} P_{cj}}\, C_{cij} \\ &= P_{c1} \left(\sum_{i=1}^{L} \gamma_i^2 + \sum_{i=1}^{L} \sum_{\substack{j=1 \\ i \neq j}}^{L} \gamma_i \gamma_j C_{cij} \right) \end{aligned} \tag{6.5-7}$$

and

$$\sigma_c^2 = B \sum_{i=1}^{L} \beta_i^2 N_{0i} \tag{6.5-8}$$

where

$$C_{c\,i\,j} = \mathbf{E}\left\{e^{j[\Delta\phi_{c,i1}(t_k)-\Delta\phi_{c\,j1}(t_k)]}\right\}$$
$$= \begin{cases} \{e^{-(1/2)[\sigma^2_{\Delta\phi_{c\,i1}}+\sigma^2_{\Delta\phi_{c\,j1}}]}, & i \neq j, \sigma^2_{\Delta\phi_{c\,11}} \equiv 0 \\ 1, & i = j \end{cases} \tag{6.5-9}$$

and

$$\sigma^2_{\Delta\phi_{c\,i\,j}} = \frac{1}{\mathrm{SNR}_{c\,i\,j}} \tag{6.5-10}$$

To illustrate the results with a simple example, let $P_{c\,i} = P_{c1}$, $N_{0\,i} = N_{01}$, and $\beta_i = 1$ for all antennas; then the signal and noise powers of the real process at the output of the carrier combiner become, respectively,

$$P_c = P_{c1}\left[L + 2(L-1)e^{-\sigma^2_{\Delta\phi,c}/2} + (L-2)(L-1)e^{-\sigma^2_{\Delta\phi,c}}\right] \tag{6.5-11}$$

$$\sigma^2_{\Delta\phi,c} = B\,L\,N_{01}$$

resulting in a correlator SNR:

$$\mathrm{SNR}_c = \frac{P_c}{\sigma^2_{\Delta\phi,c}}$$
$$= \frac{P_{c1}\left[L + 2(L-1)e^{-\sigma^2_{\Delta\phi,c}/2} + (L-2)(L-1)e^{-\sigma^2_{\Delta\phi,c}}\right]}{B\,L\,N_{01}} \tag{6.5-12}$$

In an ideal scenario, $\sigma^2_{\Delta\phi,c} \to 0$ and

$$\mathrm{SNR}_{c,\mathrm{ideal}} = \frac{P_{c1}\,L}{N_{01}\,B} \tag{6.5-13}$$

as expected. The combining degradation in dB for IF carrier arraying becomes

$$D_{ifc} = 10\log_{10}\left[\frac{\left[L + 2(L-1)e^{-\sigma^2_{\Delta\phi,c}/2} + (L-2)(L-1)e^{-\sigma^2_{\Delta\phi,c}}\right]}{L^2}\right] \tag{6.5-14}$$

References

[1] D. H. Rogstad, "Suppressed Carrier Full-Spectrum Combining," *The Telecommunications and Data Acquisition Progress Report 42-107, July–September 1991*, Jet Propulsion Laboratory, Pasadena, California, pp. 12–20, November 15, 1991. http://ipnpr.jpl.nasa.gov/progress_report/

[2] R. M. Hjellming, ed., *An Introduction to the NRAO Very Large Array*, National Radio Astronomy Observatory, Socorro, New Mexico, April 1993.

[3] D. Divsalar, "Symbol Stream Combining Versus Baseband Combining for Telemetry Arraying," *The Telecommunications and Data Acquisition Progress Report 42-74, April–June 1983*, Jet Propulsion Laboratory, Pasadena, California, pp. 13–28, August 15, 1983.

http://ipnpr.jpl.nasa.gov/progress_report/

[4] W. Hurd, J. Rabkin, M. D. Russell, B. Siev, H. W. Cooper, T. O. Anderson, and P. U. Winter, "Antenna Arraying of Voyager Telemetry Signals by Symbol Stream Combining," *The Telecommunications and Data Acquisition Progress Report 42-86, April–June 1986*, Jet Propulsion Laboratory, Pasadena, California, pp. 132–142, August 15, 1986.

http://ipnpr.jpl.nasa.gov/progress_report/

[5] D. Divsalar, "Symbol Stream Combining Versus Baseband Combining for Telemetry Arraying," *The Telecommunications and Data Acquisition Progress Report 42-74, April–June 1983*, Jet Propulsion Laboratory, Pasadena, California, pp. 13–28, August 15, 1983.

http://ipnpr.jpl.nasa.gov/progress_report/

[6] M. K. Simon and A. Mileant, *Performance Analysis of the DSN Baseband Assembly Real-Time Combiner*, JPL Publication 84-94, Rev. 1, May 1, 1985.

[7] D. Divsalar and J. H. Yuen, "Improved Carrier Tracking Performance with Coupled Phase-Locked Loops," *The Telecommunications and Data Acquisition Progress Report 42-66, September and October 1981*, Jet Propulsion Laboratory, Pasadena, California, pp. 148–171, December 15, 1981. http://ipnpr.jpl.nasa.gov/progress_report/